Evidence for Strong Mixing between the LC and MLCT Excited States in Bis(2-phenylpyridinato-C^2,N')(2,2'-bipyridine)iridium(III)

Mirco G. Colombo, Andreas Hauser, and Hans U. Güdel*

Institut für Anorganische, Analytische und Physikalische Chemie, Universität Bern, Freiestrasse 3, 3000 Bern 9, Switzerland

Received March 10, 1993

The well-resolved absorption, excitation, and luminescence spectra of $[Ir(ppy)_2bpy]^+$ (ppyH = 2-phenylpyridine, bpy = 2,2'-bipyridine) in different media at cryogenic temperatures are presented. In solutions and glasses at ambient temperature the lowest energy excited state corresponds to an Ir → bpy charge-transfer excitation whereas in the crystalline host lattice $[Rh(ppy)_2bpy]PF_6$ the lowest excited state at 21 450 cm^{-1} is assigned to a $^3\pi-\pi^*$ excitation localized on the cyclometalating ppy^- ligands. The next higher excited Ir → bpy charge-transfer state has shifted to 21 820 cm^{-1}, only 300 cm^{-1} above the ^{3}LC excited state. The close proximity of the ^{3}LC and ^{3}MLCT excited states and the large spin–orbit coupling constant of Ir^{3+} induce a strong mixing of charge-transfer character into the ^{3}LC lowest excited states, resulting in increased oscillator strengths, reduced lifetimes, short axis polarized transitions, and a large zero-field splitting of 10–15 cm^{-1}.

1. Introduction

Most recent reports on the synthesis of cyclometalated Rh^{3+} [1-3] and Ir^{3+} [4-10] complexes include an attempt to identify the nature of their lowest excited states, because these states are mainly responsible for the interesting photochemical and photocatalytic properties. The classification into ligand centered (LC) $\pi-\pi^*$ and metal to ligand charge-transfer (MLCT) transitions is normally made on the basis of luminescence lifetimes and band shapes, whereas the active ligand in mixed-ligand complexes is identified by electrochemical measurements.

Quite often room-temperature solution spectra are sufficient for such a classification, but in some cases, especially when the LC and MLCT excited states lie close to each other, solid-state spectroscopic methods at cryogenic temperatures have to be applied. Both luminescence[11-13] and excitation[14,15] line narrowing as well as single crystal absorption[10,16] spectroscopy have proven to be most valuable for the investigation of a series of cyclometalated Rh^{3+} and Ir^{3+} complexes. In the complexes $[Rh(ppy)_2bpy]^+$ (ppyH = 2-phenylpyridine, bpy = 2,2'-bipyridine)[16] and $[Rh(thpy)_2bpy]^+$ (thpyH = 2-(2-thienyl)pyridine)[13] the lowest energy excited states are localized on the individual ligands and have essentially $^3\pi-\pi^*$ character. In both complexes the $^3\pi-\pi^*$ excited states of the cyclometalating ligands lie below the $^3\pi-\pi^*$ excited state centered on bpy. In the Ir analogue $[Ir(thpy)_2bpy]^+$ the lowest excited states in solid hosts still correspond to $^3\pi-\pi^*$ transitions on the $thpy^-$ ligands but the Ir → bpy CT state has shifted below the $^3\pi-\pi^*$ state of bpy.[10] In addition, the oscillator strengths, luminescence lifetimes, and vibrational structure of the $^3\pi-\pi^*$ transitions reflect a substantial mixing of LC and MLCT character.

If $thpy^-$ is replaced by ppy^-, the ligand centered transitions lie at higher energy and we expect a further stabilization of the MLCT excited states. In this work we show that this may lead to a reversal in the order of the lowest excited LC and MLCT states in the title compound and that there is substantial mixing between these states. We report luminescence spectra of $[Ir(ppy)_2bpy]^+$ dissolved in CH_2Cl_2, embedded in poly(methyl methacrylate) and doped into $[Rh(ppy)_2bpy]PF_6$ as well as excitation and absorption spectra of the latter down to liquid-helium temperature.

2. Experimental Section

The synthesis of $[Rh(ppy)_2bpy]PF_6$ and $[Ir(ppy)_2bpy]PF_6$ has been reported in the literature.[3,4,6] We used the slightly modified procedure described in ref 10 for the $[Ir(thpy)_2bpy]^+$ complex.

$[Ir(ppy)_2bpy]PF_6$ was imbedded in poly(methyl methacrylate) (PMMA) by dissolving the salt in dichloromethane and adding this solution to a solution of 8% PMMA in dichloromethane. Glasses were obtained by slow evaporation of the solvent. Doped crystals were prepared by dissolving the host and guest complex together in methanol followed by cocrystallization of the complexes by slow solvent exchange with diethyl ether. $[Rh(ppy)_2bpy]PF_6$ and $[Ir(ppy)_2bpy]PF_6$ were found to be isostructural. Mixed crystals $[Rh_{1-x}Ir_x(ppy)_2bpy]PF_6$ with $0 \le x \le 1$ can be prepared for any value of x. The results presented here were obtained on samples with a low doping level ($x = 2.8 \times 10^{-3}$). The doped $[Rh(ppy)_2bpy]PF_6$ crystallized in pseudohexagonal needles with typical dimensions of about 1 mm × 0.2 mm × 0.1 mm, where the needle axis corresponds to the $\vec{b}$-axis of the orthorhombic unit cell.[16]

The samples used for single-crystal absorption were chosen by observation of their behavior between crossed polarizers with an Olympus SZ4045 stereo microscope. Measurements were made with the light propagating parallel to the $\vec{a}$ (polarized parallel $\vec{b}$ and $\vec{c}$, respectively) and $\vec{c}$ (polarized parallel $\vec{a}$ and $\vec{b}$, respectively) axes, respectively.

Room-temperature luminescence spectra of solutions were measured on a commercial spectrofluorometer (Spex FluoroMax). The equipment used for high-resolution spectroscopic measurements at cryogenic temperatures has been described previously.[10]

3. Results

The luminescence spectra of $[Ir(ppy)_2bpy]PF_6$ in different media are shown in Figure 1. The room-temperature lumine-

(1) Mäder, U.; Jenny, T.; von Zelewsky, A. *Helv. Chim. Acta* **1986**, *69*, 1085.
(2) van Diemen, J. H.; Haasnoot, J. G.; Hage, R.; Reedijk, J.; Vos, J. G.; Wang, R. *Inorg. Chem.* **1991**, *30*, 4038.
(3) Maeder, U.; von Zelewsky, A.; Stoeckli-Evans, H. *Helv. Chim. Acta* **1992**, *75*, 1320.
(4) Sprouse, S.; King, K. A.; Spellane, P. J.; Watts, R. J. *J. Am. Chem. Soc.* **1984**, *106*, 6647.
(5) King, K. A.; Spellane, P. J.; Watts, R. J. *J. Am. Chem. Soc.* **1985**, *107*, 1431.
(6) King, K. A.; Watts, R. J. *J. Am. Chem. Soc.* **1987**, *109*, 1589.
(7) Ohsawa, Y.; Sprouse, S.; King, K. A.; DeArmond, M. K.; Hanck, K. W.; Watts, R. J. *J. Phys. Chem.* **1987**, *91*, 1047.
(8) Garces, F. O.; Watts, R. J. *Inorg. Chem.* **1990**, *29*, 583.
(9) Dedeian, K.; Djurovich, P. I.; Garces, F. O.; Carlson, G.; Watts, R. J. *Inorg. Chem.* **1991**, *30*, 1685.
(10) Colombo, M. G.; Güdel, H. U. *Inorg. Chem.*, preceding paper in this issue.
(11) Colombo, M. G.; Zilian, A.; Güdel, H. U. *J. Am. Chem. Soc.* **1990**, *112*, 4581.
(12) Colombo, M. G.; Zilian, A.; Güdel, H. U. *J. Lumin.* **1991**, *48*, *49*, 549.
(13) Zilian, A.; Güdel, H. U. *Inorg. Chem.* **1992**, *31*, 830.
(14) Zilian, A.; Güdel, H. U. *Coord. Chem. Rev.* **1991**, *111*, 33.
(15) Zilian, A.; Güdel, H. U. *J. Lumin.* **1992**, *51*, 237.
(16) Frei, G.; Zilian, A.; Raselli, A.; Güdel, H. U.; Bürgi, H. B. *Inorg. Chem.* **1992**, *31*, 4766.

0020-1669/93/1332-3088$04.00/0

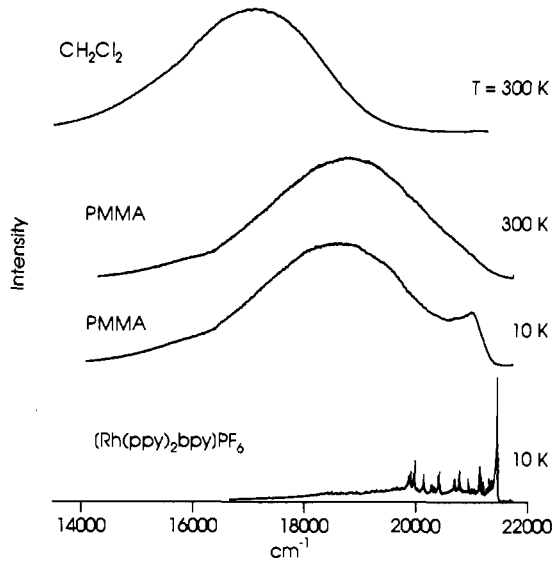

Figure 1. Luminescence spectra of [Ir(ppy)$_2$bpy]PF$_6$ in different media, excitation at 457.9 nm. The title complex was dissolved in CH_2Cl_2 (10^{-5} M) in the case of the upper spectrum or embedded in poly(methyl methacrylate) (PMMA, 10^{-3} M) or doped into the crystal lattice of [Rh(ppy)$_2$bpy]PF$_6$ (0.28%) for the lower spectra.

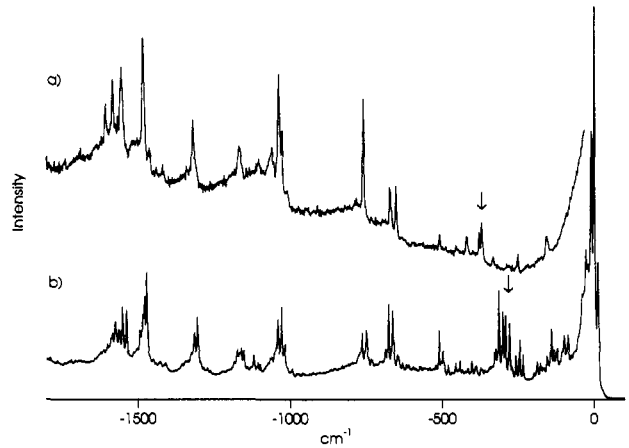

Figure 2. Comparison of the low-temperature luminescence spectra of [Rh(ppy)$_2$bpy]$^+$ (a) and [Ir(ppy)$_2$bpy]$^+$ (b), displayed relative to their origins. (a) is the luminescence line narrowing spectrum of [Rh(ppy)$_2$bpy]$^+$ in a nitrile glass at T = 6 K, excitation at 457.9 nm;[11] (b) is the spectrum of [Ir(ppy)$_2$bpy]$^+$ doped (0.28%) into [Rh(ppy)$_2$bpy]PF$_6$ at T = 10 K, excitation at 457.9 nm. The arrows indicate vibrational sidebands, which are distinctive for the Rh^{3+} and Ir^{3+} spectra.

scence spectrum in dichloromethane consists of a broad structureless band with its maximum at 17 090 cm^{-1}. The room-temperature luminescence spectrum in PMMA is similar, but the band has significantly shifted to higher energy and is now centered at 18 780 cm^{-1}. At 10 K the PMMA spectrum is still governed by the broad band which has slightly red shifted to 18 550 cm^{-1}, but in addition there is a shoulder showing up at 21 000 cm^{-1}. The luminescence spectrum changes its appearance completely when the complex is built into a crystalline host. Doped (0.28%) into [Rh(ppy)$_2$bpy]PF$_6$ at 10 K it is characterized by a prominent electronic origin line at 18 452 cm^{-1} and well-resolved vibrational sidebands.

In Figure 2 the luminescence line narrowing spectrum of [Rh(ppy)$_2$bpy]PF$_6$ in a nitrile glass (a)[11] and the luminescence spectrum of [Ir(ppy)$_2$bpy]PF$_6$ doped into [Rh(ppy)$_2$bpy]PF$_6$ (b) are compared on an energy scale relative to their respective electronic origins. Above 500 cm^{-1} the vibrational sideband patterns of the two complexes are very similar. Almost every vibrational band in the [Rh(ppy)$_2$bpy]PF$_6$ spectrum has a counterpart in the [Ir(ppy)$_2$bpy]PF$_6$ spectrum. Below 400 cm^{-1}, however, the Ir^{3+} complex shows a number of intense sidebands

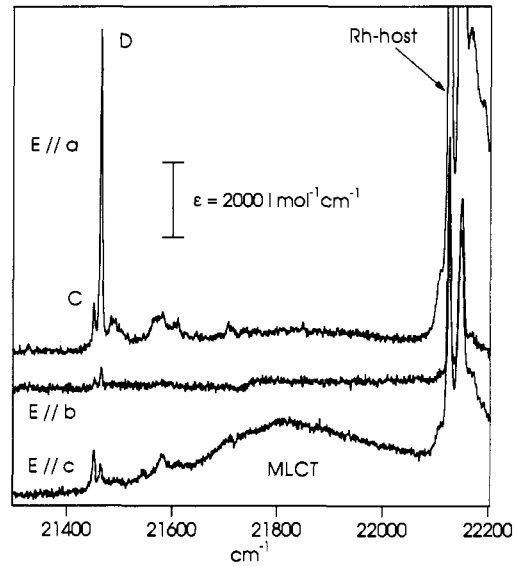

Figure 3. Polarized single-crystal absorption spectra at T = 12 K of [Ir(ppy)$_2$bpy]PF$_6$, doped into [Rh(ppy)$_2$bpy]PF$_6$ (0.28%). The spectra were recorded with the electric field vector parallel to the $\vec{a}$-, $\vec{b}$-, and $\vec{c}$-axes of the crystal, respectively. The labels C, D, and MLCT are explained in the text. The onset of the host absorption is marked by an arrow.

(see arrows in Figure 2) which are shifted to lower energy with respect to the Rh^{3+} complex. A second distinctive feature is the splitting of about 12 cm^{-1} of the electronic origin as well as of the vibrational sidebands in the Ir^{3+} complex. The origin region of the Ir^{3+} spectrum carries approximately 11% of the total band intensity.

Polarized single-crystal absorption spectra at T = 12 K of [Ir(ppy)$_2$bpy]PF$_6$ doped (0.28%) into [Rh(ppy)$_2$bpy]PF$_6$ are presented in figure 3. The sharp bands at 22 126 and 22 148 cm^{-1} are the origins of the [Rh(ppy)$_2$bpy]PF$_6$ host, the absorption behavior of which has been described elsewhere.[16] Therefore we will concentrate on the lower energy absorption bands which are caused by [Ir(ppy)$_2$bpy]$^+$. Two sharp origins C and D at 21 452 and 21 465 cm^{-1}, respectively, and a broad band called MLCT with its maximum at 21 820 cm^{-1} can be identified. In the $E\|\vec{a}$ spectrum the typical sideband structure built on the strong origin D can be recognized.

The dichroic ratios of the three bands are quite different: while band C is about equally intense for light polarized parallel to the $\vec{a}$- and the $\vec{c}$-axes of the crystal, the polarization of the D band is mainly parallel $\vec{a}$, and the MLCT band is most intense for $E\|\vec{c}$. The sharp bands C and D still have well observable transition moments with $E\|\vec{b}$, whereas the absorption of the MLCT band vanishes for this polarization. The oscillator strengths of the absorption bands can be deduced from the spectrum according to[17]

$$f_{ij}^{q} = 4.32 \times 10^{-9} \int_{\text{abs band}} \epsilon(\tilde{\nu})\, d\tilde{\nu} \qquad (1)$$

where $\epsilon(\tilde{\nu})$ is the extinction coefficient in q polarization and the energy scale is in cm^{-1}. An average oscillator strength f_{ij}(ed) for an electric dipole allowed transition between the states i and j can be defined as follows:[18]

$$f_{ij}(\text{ed}) = {}^1/_3[f_{ij}^{x}(\text{ed}) + f_{ij}^{y}(\text{ed}) + f_{ij}^{z}(\text{ed})] \qquad (2)$$

The extinction coefficients and oscillator strengths of the bands derived by using eqs 1 and 2 are listed in Table I. The total

(17) Schäfer, H. L.; Gliemann, G. *Einführung* in die Ligandenfeldtheorie, Akademische Verlagsgemeinschaft: Frankfurt a. M., Germany, 1967; p 92.
(18) Imbusch, G. F. In *Luminescence Spectroscopy*; Lumb, M. D., Ed.; Academic Press: London, 1987; pp 1–92.

Table I. Extinction Coefficients and Oscillator Strengths of the Lowest-Energy Excitations of $[Ir(ppy)_2bpy]PF_6$ Doped into $[Rh(ppy)_2bpy]PF_6$

	C band			D band			MLCT band	
polarization	ϵ_{max}(origin) (L mol^{-1} cm^{-1})	f(origin)	f(tot. band)	ϵ_{max}(origin) (L mol^{-1} cm^{-1})	f(origin)	f(tot. band)	ϵ_{max} (L mol^{-1} cm^{-1})	f
$\vec{E}\parallel\vec{a}$	1546	7.10×10^{-5}	6.45×10^{-4}	7673	3.11×10^{-4}	2.83×10^{-3}	772	1.74×10^{-3}
$\vec{E}\parallel\vec{b}$	205	8.11×10^{-6}	7.37×10^{-5}	562	2.10×10^{-5}	1.91×10^{-4}	≤ 33	$\leq 7.39 \times 10^{-5}$
$\vec{E}\parallel\vec{c}$	963	4.73×10^{-5}	4.30×10^{-4}	604	1.89×10^{-5}	1.72×10^{-4}	1491	3.23×10^{-3}
av	905	4.21×10^{-5}	3.82×10^{-4}	2946	1.17×10^{-4}	1.06×10^{-3}	765	1.68×10^{-3}

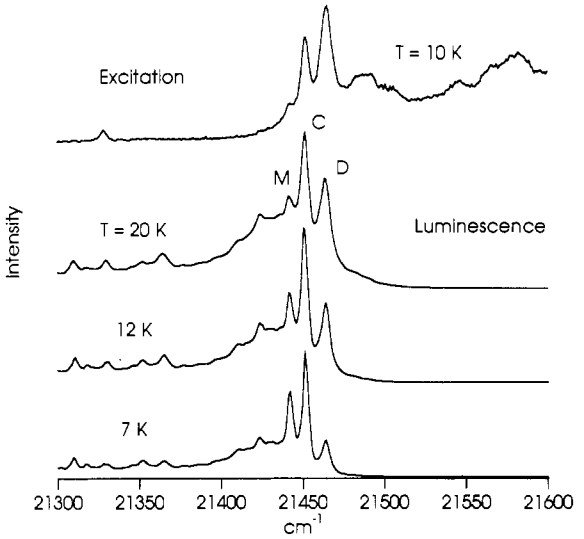

Figure 4. Origin region of the low-temperature excitation (luminescence monitored broad band below (20 200 cm^{-1}) and luminescence (excitation at 457.9 nm with an Ar laser) spectra of $[Ir(ppy)_2bpy]PF_6$ in $[Rh(ppy)_2bpy]PF_6$. M, C, and D label electronic origins.

intensities of the sharp absorption bands C and D were calculated under the assumption that the origins carry ≈11% of the respective band intensities as they do in luminescence.

The origin region of the low-temperature excitation and luminescence spectra of $[Ir(ppy)_2bpy]PF_6$ doped (0.28%) into $[Rh(ppy)_2bpy]PF_6$ is shown in Figure 4. The sharp bands C and D at 21 452 and 21 465 cm^{-1}, respectively, coincide with the respective origins of the absorption spectra. A third band labeled M at 21 442 cm^{-1} appears in the luminescence spectra at the lowest temperatures. It can also be seen in the excitation spectrum and as shoulder in the absorption spectra of higher doped samples. The intensity distribution between the three origin lines is temperature dependent: The band D grows, the band C remains roughly constant, and the band M tends to decrease with increasing temperature. The temperature dependence of the M band is not that obvious, because the underlying phonon wings of C and D obscure the situation. Selective excitation into each of the three origins resulted in basically the same luminescence spectrum.

4. Discussion

4.1. Assignment of the Lowest Excited States. Because of their band shape and solvent-dependent red shifts, the broad structureless luminescence bands in Figure 1 can be assigned to MLCT transitions,[6] whereas the structured luminescence band with a small Stokes shift of the title complex doped into $[Rh(ppy)_2bpy]PF_6$ is typical for ligand-centered $^3\pi-\pi^*$ transitions. Thus either a ^{3}LC or a ^{3}MLCT is the lowest excited state depending on the environment. In solutions and glasses at room temperature the ^{3}MLCT is stabilized with respect to the ^{3}LC state, while in crystalline hosts at low temperatures this order is reversed. In the low-temperature spectrum of the PMMA glass both luminescences are superimposed. The enhanced rigidity of the host moves the ^{3}MLCT state up in energy when the temperature is lowered. At some point it will cross the ^{3}LC state, which will then become the emitting state at 10 K. Due to the broad inhomogeneous distribution of sites in the glass, there are complexes on both sides of the crossing point. As a result we observe a superimposition of the two types of luminescences.

The vibrational sideband pattern of the ligand-centered luminescence is characteristic for a given ligand; therefore, it can be used to identify the active ligand in mixed-ligand complexes.[10-13] In the previously investigated $[Rh(ppy)_2bpy]^+$, $[Rh(thpy)_2bpy]^+$, and $[Ir(thpy)_2bpy]^+$ the lowest ^{3}LC state was always found to be localized on the cyclometalating ligands.[10-16] The similarity of the sideband patterns of $[Rh(ppy)_2bpy]^+$ and $[Ir(ppy)_2bpy]^+$ in Figure 2 indicates that for $[Ir(ppy)_2bpy]^+$, too, the lowest excited ^{3}LC state is centered on the ppy^- ligands.

This assignment is confirmed by the single-crystal absorption spectra displayed in Figure 3. For each of the three absorption bands C, D, and MLCT, the components of the transition moment with respect to the symmetry axes of the complex can be calculated by making use of the dichroic ratios in Table I and the crystal structure of the $[Rh(ppy)_2bpy]PF_6$ host.[16] Following the procedure given in ref 16, it can be shown that the lines C and D are compatible with exclusively short axis polarized transitions on the two crystallographically inequivalent ppy^- ligands. On the basis of their narrow bandwidth and the coincidence of the lines C and D in absorption and luminescence, we assign C and D to $^3\pi-\pi^*$ excitations localized on the crystallographically inequivalent ppy^- ligands, in analogy to the related $[Rh(ppy)_2bpy]^+$ [16] and $[Ir(thpy)_2bpy]^+$ [10] systems.

The band shape and oscillator strength of the broad band at 21 820 cm^{-1} suggest that it belongs to a ^{3}MLCT transition. A similar band at almost the same energy (21 700 cm^{-1}) was found for $[Ir(thpy)_2bpy]^+$ doped into $[Rh(ppy)_2bpy]PF_6$,[10] but no corresponding band is observed for the neat host $[Rh(ppy)_2bpy]PF_6$.[16] Its polarization behavior is compatible with a transition moment along the Ir → bpy direction. As in $[Ir(thpy)_2bpy]^+$, we therefore assign it to an Ir → bpy charge-transfer transition.

4.2. Mixing between the LC and MLCT Excited States. The transitions C and D were assigned to ^{3}LC excitations because of their band shape and vibrational fine structure. But if a classification based on oscillator strength were chosen, we would have to ascribe these bands to ^{3}MLCT transitions. They are 4 orders of magnitude more intense than $^3\pi-\pi^*$ transitions in ppyH.[19] In addition their polarization within the ligand plane is in contrast to the usual out of plane polarization of $^3\pi-\pi^*$ transitions.[20,21] So from this point of view the assignment is ambiguous. By following the trend within a series of related complexes, we can clarify the situation. In the order from $[Rh(ppy)_2bpy]^+$ to $[Ir(thpy)_2bpy]^+$, the oscillator strength of the corresponding bands increases by a factor of 8, and between $[Ir(thpy)_2bpy]^+$ and $[Ir(ppy)_2bpy]^+$ we observe a further increase by an average factor of 2.8. This increase in the intensity of the nominally ligand-centered bands can be explained by a mixing between the ^{3}LC and ^{1}MLCT excited states through spin–orbit coupling. This also explains the observed in-plane polarization because the MLCT transitions are polarized in the metal to ligand direction. According to Komada et al.[22] the following relation

(19) Maestri, M.; Sandrini, D.; Balzani, V.; Maeder, U.; von Zelewsky, A. *Inorg. Chem.* **1987**, *26*, 1323.
(20) Gropper, H.; Dörr, F. *Ber. Bunsen-Ges. Phys. Chem.* **1963**, *67*, 46.
(21) DeArmond, M. K.; Huang, W. L.; Carlin, C. M. *Inorg. Chem.* **1979**, *18*, 3388.
(22) Komada, Y.; Yamauchi, S.; Hirota, N. *J. Phys. Chem.* **1986**, *90*, 6425.

between the radiative rate constants k_{rad} and the spin–orbit coupling matrix element holds:

$$\frac{k_{rad}(^3LC)}{k_{rad}(^1MLCT)} = \left(\frac{\nu(^3LC)}{\nu(^1MLCT)}\right)^3 \left(\frac{\langle ^1MLCT|H_{SO}|^3LC\rangle}{h\nu(^1MLCT) - h\nu(^3LC)}\right)^2 \quad (3)$$

where ν values are the transition frequencies. Assuming an electric dipole (ed) intensity mechanism, the radiative rate constant is related to the oscillator strength f_{ij} by[18,23]

$$f_{ij}(ed)\frac{1}{k_{rad}} = 1.5 \times 10^4 \frac{g_u}{g_l} \frac{(c/\nu)^2}{n\left(\frac{n^2+2}{3}\right)^2} \quad \text{(SI units)} \quad (4)$$

where n is the refractive index of the substance and c the vacuum velocity of light. g_l and g_u are the degeneracies of the lower and the upper state, respectively. Using eq 4, formula 3 can be rewritten in terms of oscillator strengths:

$$\frac{1}{3}\frac{f(^3LC)}{f(^1MLCT)} = \left(\frac{\nu(^3LC)}{\nu(^1MLCT)}\right)\left(\frac{\langle ^1MLCT|H_{SO}|^3LC\rangle}{h\nu(^1MLCT) - h\nu(^3LC)}\right)^2 \quad (5)$$

where the factor of $^1/_3$ comes from the spin multiplicity. The spin–orbit coupling constant of Ir^{3+} is about 50% larger than the one of Rh^{3+}.[24] For the energy of the ^{3}LC transition of [Ir(ppy)$_2$bpy]$^+$ the spectral position of the sharp origin lines at ≈21 450 cm^{-1} is taken. In first order the $^3\pi$–π^* transitions on the cyclometalating ligands get their intensity by mixing with the ^{1}MLCT state involving the same ligand. Therefore the energy of ≈25 000 cm^{-1} for the ^{1}MLCT (Ir → ppy$^-$) transition was taken from the absorption spectrum of the dichloro-bridged dimer [Ir(ppy)$_2$Cl]$_2$,[4] because in the absorption spectrum of the monomer [Ir(ppy)$_2$bpy]$^+$ the discrimination between the bands belonging to Ir → bpy and Ir → ppy$^-$ CT transitions is difficult. It should be noted that the MLCT transition energies in the crystal are blue shifted with respect to the ones in dichloromethane solution we use for the calculation here, but the solution values are sufficient for our rough estimate. For [Ir(thpy)$_2$bpy]$^+$ and [Rh(ppy)$_2$bpy]$^+$ the energy gap between the ^{3}LC and ^{1}MLCT transitions of the cyclometalating ligands is about the same, and it is about 1.5 times larger than the one for [Ir(ppy)$_2$bpy]$^+$. With these values we calculate an intensity increase of a factor of 2 between [Rh(ppy)$_2$bpy]$^+$ and [Ir(thpy)$_2$bpy]$^+$ and of a factor of 2.6 between [Ir(thpy)$_2$bpy]$^+$ and [Ir(ppy)$_2$bpy]$^+$, respectively. The calculation thus reproduces the observed intensity increase between the Ir^{3+} complexes but underestimates the increase between the Rh^{3+} and the Ir^{3+} complexes. This indicates that not only the change in the spin–orbit coupling constant but also the change in the wave functions between the Rh^{3+} and the Ir^{3+} complex enters into the matrix element. The band shape is hardly affected by the mixing between the ^{3}LC and ^{1}MLCT states, and therefore additional properties such as band intensities and polarizations are essential for a proper characterization.

In all the investigated complexes, including the Rh complexes, the nominally ^{3}LC transitions get most of their intensity through the discussed mixing with the ^{1}MI CT states. Therefore these $^3\pi$–π^* transitions are all polarized within the ligand plane.[16] The transition moments of the weakly mixed ^{3}LC(ppy$^-$) transitions in [Rh(ppy)$_2$bpy]$^+$ [16] are almost parallel to the Rh–N(ppy$^-$) bonds. In the stronger mixed [Ir(thpy)$_2$bpy]$^+$ the corresponding transitions on the thpy$^-$ have turned within the ligand plane by about 10° toward the short axis direction, and in the title compound [Ir(ppy)$_2$bpy]$^+$ the strongly mixed ^{3}LC(ppy$^-$) transitions are completely short axis polarized.

Another indication for the mixing between the ^{3}LC and ^{1}MLCT states is the behavior of the low-energy vibrational sidebands ($\nu \leq 400$ cm^{-1}) in the luminescence spectra. This energy range is typical for metal–ligand vibrations,[25] and calculations have shown[26] that these vibrations carry indeed a considerable amount of metal–ligand character. The occurrence of metal–ligand vibrational sidebands in nominally ligand-centered transitions is a manifestation of their increased charge-transfer character.[10] The more metal–ligand character a vibration has, the larger the frequency shift expected, when a metal is replaced by another one with a different mass. This can be seen in the vibrational sidebands marked with an arrow in Figure 3. Corresponding bands are shifted to lower frequencies in the Ir^{3+} complex due to the bigger mass of Ir^{3+}. Furthermore there is an enormous increase in the intensity of the metal–ligand vibrational sidebands in the strongly mixed [Ir(ppy)$_2$bpy]$^+$.

4.3. Zero-Field Splittings. The last problem we are confronted with is the additional splitting of the origins C and D in [Ir(ppy)$_2$bpy]$^+$ doped into [Rh(ppy)$_2$bpy]PF$_6$. There is the line M in Figure 4, lying 10 cm^{-1} below the line C, and we have to assume that a corresponding line belonging to D is buried under line C. Such splittings have not been observed in [Rh(ppy)$_2$bpy]PF$_6$. The fact that the luminescence spectra are independent of selective excitation into the different origins and the temperature dependence of the intensity ratios between the three origin lines shows that we are dealing with an electronic splitting and not with complexes on different crystal sites, as it is often the case in crystal spectroscopy.[27] What are the reasons of this splitting? The mixing of ^{1}MLCT character into ^{3}LC states can drastically increase the zero-field splittings (ZFS). The contribution of the mixing between the ^{3}LC and ^{1}MLCT states to the ZFS is given by the second-order perturbation expression:[22]

$$ZFS(^3LC) = |\langle ^1MLCT|H_{SO}|^3LC\rangle|^2 \left(\frac{1}{h\nu(^3MLCT) - h\nu(^3LC)} - \frac{1}{h\nu(^1MLCT) - h\nu(^3LC)}\right) \quad (6)$$

The matrix element can be evaluated with formula 5. From Table I we get an average oscillator strength for the transitions C and D of $f_{ij}(^3LC) \approx 7 \times 10^{-4}$. The oscillator strength of the ^{1}MLCT transitions of such complexes is typically 0.1.[22] Using the above values, the ^{1}MLCT (Ir → ppy$^-$) transition energy of 25 000 cm^{-1} of section 4.2, and an estimate for the ^{3}MLCT (Ir → ppy$^-$) transition energy of 23 000 cm^{-1}, also taken from the solution absorption spectrum of [Ir(ppy)$_2$Cl]$_2$, we calculate a matrix element $|\langle ^1MLCT|H_{SO}|^3LC\rangle| \approx 190$ cm^{-1} and a zero-field splitting ZFS of ≈13 cm^{-1} in very good agreement with the observed splittings of the C and D origins in Figure 4. This splitting is very large compared to the one of the related Rh^{3+} compounds for which ODMR[22,28] measurements gave a ZFS in the range of 0.1 cm^{-1}, i.e. 2 orders of magnitude smaller than the splitting observed here. Riesen and Krausz estimated a ZFS of 3 cm^{-1} for [Ir(5,6-Me$_2$phen)$_2$Cl$_2$]$^+$.[29] This complex still shows a typical ^{3}LC luminescence band shape in a glassy matrix, and therefore its emitting state has less charge-transfer character than [Ir(ppy)$_2$bpy]$^+$.

The large ZFS in the title compound is supported by the luminescence lifetimes, which decrease from about 140 μs at 5

(23) McGlynn, S. P.; Azumi, T.; Kinoshita, M. *Molecular Spectroscopy of the Triplet State*; Prentice-Hall: Englewood Cliffs, NJ, 1969; p 17.
(24) Abragam, A.; Bleaney, B. *Electron Paramagnetic Resonance of Transition Ions*; Clarendon Press: Oxford, U.K., 1970; p 474.
(25) Nakamoto, K. *Infrared and Raman Spectra of Inorganic and Coordination Compounds*, 4th ed.; Wiley-Interscience: New York, 1986; pp 208–213.
(26) Strommen, D. P.; Malick, P. K.; Danzer, G. D.; Lumpkin, R. S.; Kincaid, J. R. *J. Phys. Chem.* **1990**, *94*, 1357.
(27) Braun, D.; Gallhuber, E.; Hensler, G.; Yersin, H. *Mol. Phys.* **1989**, *67*, 417.
(28) Giesbergen, C. P. M.; Sitters, R.; Frei, G.; Zilian, A.; Güdel, H. U.; Glasbeek, M. *Chem. Phys. Lett.* **1992**, *197*, 451.
(29) Riesen, H.; Krausz, E. *J. Lumin.* **1992**, *53*, 263.
(30) Zilian, A.; Frei, G.; Güdel, H. U. *Chem. Phys.*, in press.

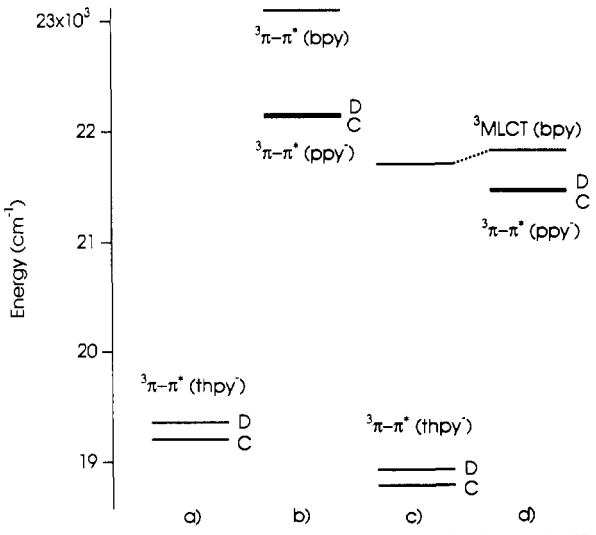

Figure 5. Energies and classification of the first excited states in $[Rh(thpy)_2bpy]^+$ (a),[30] $[Rh(ppy)_2bpy]^+$ (b),[16] $[Ir(thpy)_2bpy]^+$ (c),[10] and $[Ir(ppy)_2bpy]^+$ (d) in the crystal lattice of $[Rh(ppy)_2bpy]PF_6$.

K to 3 μs at 100 K. The decay curves are not single exponentials at low temperatures due to a slowdown of spin–lattice relaxation rates, but the above values are good estimates of the "average" lifetimes. Since the luminescence intensities stay constant between 5 and 100 K, the significant drop in lifetime, which is not observed in the corresponding Rh^{3+} complex, is due to an increase in the radiative decay rate. We attribute this to a thermal population in this temperature range of the higher spin sublevels of the states C and D. This is in analogy to $[Rh(phen)_3]^{3+}$ and $[Rh(bpy)_3]^{3+}$ where the transitions to the various spin sublevels were found to have significantly different oscillator strengths from each other, too.[22] Between 100 and 295 K the luminescence lifetime of $[Ir(ppy)_2bpy]^+$ doped into $[Rh(ppy)_2bpy]PF_6$ drops from 3 μs to below 100 ns. This decrease is accompanied by a corresponding decrease of the intensity to 3% and thus is clearly due to an opening of thermally activated nonradiative decay channels.

5. Comparison with Related Complexes and Conclusions

We can gain a great deal of insight into the nature of the first excited states in mixed-ligand cyclometalated Rh^{3+} and Ir^{3+} complexes by comparing their properties within a series of related compounds. In Figure 5 we show how the energies of the first excited states vary within the series $[Rh(thpy)_2bpy]^+$, $[Rh(ppy)_2bpy]^+$, $[Ir(thpy)_2bpy]^+$, and $[Ir(ppy)_2bpy]^+$. In all complexes, when embedded in the $[Rh(ppy)_2bpy]PF_6$ lattice, transitions involving the bpy ligand lie at higher energies than the nominally $^3\pi-\pi^*$ transitions centered on the cyclometalating ligands. In the two Ir^{3+} complexes the first charge-transfer transition, which corresponds to an Ir → bpy electron transfer, has moved down in energy to come close to the first excited states. The energy of this first ^{3}MLCT state strongly depends on the environment, and in fluid solution it is the emitting state in both $[Ir(thpy)_2bpy]^+$ and $[Ir(ppy)_2bpy]^+$. In PMMA the title complex shows dominant ^{3}MLCT emission down to low temperatures, whereas $[Ir(thpy)_2bpy]^+$ keeps its $^3\pi-\pi^*$ emitter characteristics up to room temperature. We thus have the following very interesting situation. The two competing states have not only different characters, one is nominally ligand centered while the other charge transfer, but they involve different ligands.

Why are the first nominally $^3\pi-\pi^*$ transitions localized on the cyclometalating ligands, while the first charge-transfer transition involves the bpy ligand? An extended Hückel calculation on $[Rh(ppy)_2bpy]^+$ clearly places the bpy unoccupied orbitals below the ppy^- unoccupied orbitals.[31] This is the order for the ^{3}MLCT transitions, and it is also the order derived from cyclic voltammograms of $[Ir(thpy)_2bpy]^+$ [10] and $[Ir(ppy)_2bpy]^+$.[7] If we want to rationalize the relative $^3\pi-\pi^*$ energies, however, a one electron model is insufficient. The important factor here is the singlet–triplet energy splitting in a $\pi-\pi^*$ excitation. This splitting is on the order of ≈11 000 cm^{-1} in $[Rh(ppy)_2bpy]^+$ and $[Ir(ppy)_2bpy]^+$ and ≈14 000 cm^{-1} in $[Rh(thpy)_2bpy]^+$ and $[Ir(thpy)_2bpy]^+$, respectively. It is mainly determined by exchange integrals which are strongly dependent on the electronic wave functions of the π and π^* orbitals. In $thpy^-$ these integrals are significantly larger than in ppy^-, thus pushing the first $^3\pi-\pi^*$ states down to ≈19 000 cm^{-1} in both $[Rh(thpy)_2bpy]^+$ and $[Ir(thpy)_2bpy]^+$; See Figure 5.

Let us finally return to the question of how to characterize the emitting state of $[Ir(ppy)_2bpy]^+$. In fluid solution at room temperature the answer is clear: it is an Ir → bpy ^{3}MLCT state. In the crystalline host $[Rh(ppy)_2bpy]PF_6$ at 10 K the answer depends on the property we use for the classification. On the basis of its band shape it is a ligand centered $^3\pi-\pi^*$ state. On the basis of its polarization, intensity, lifetime, and zero-field splitting it has charge-transfer character. This is not a contradiction as it might appear at first sight; it simply reflects the limitations of the usual classification scheme in the present situation. Since the band shape is very distinctive, it is practical to use it even in this borderline situation. But we have to keep in mind that the label $^3\pi-\pi^*$ has a completely different meaning in the title complex and in the free ppyH ligand. Its oscillator strength is about 4 orders of magnitude bigger in the complex due to mixed-in charge-transfer character, and it is remarkable that this has virtually no effect on the band shape.

Acknowledgment. We thank R. J. Watts for initially providing a sample of $[Ir(ppy)_2bpy]Cl$. $IrCl_3$ was generously provided as a loan by Johnson-Matthey. Financial support by the Swiss National Science Foundation is gratefully acknowledged.

(31) Zilian, A. Unpublished results.